Noname manuscript No.
(will be inserted by the editor)

Image Selective Segmentation Model for Multi-Regions within the Object of Interest with Application to Medical Disease

Haider Ali · Shah Faisal · Ke Chen · Lavdie Rada

Received: date / Accepted: date

Abstract Detection and extraction of an object of interest and accurate boundaries segmentation in a given image has been of interest in the last decades due to its application in different fields. To successfully segment a single object, interactive/selective segmentation techniques has been developed as a supplement to the existing global segmentation techniques. Even though existing interactive/ selective segmentation techniques perform well in segmenting the images with prominent edges those methods are less efficient or even fail in segmenting images having muti-regions of different intensity scale. In this paper, we design a new variational selective segmentation model which incorporates the idea of area-based fitting term along with a signed pressure force function based on a generalized average into a variational energy function. The new model is capable to capture the object of interest which can be single or multi-region within the object of interest. To evaluate the performance of our new model, we compare our results with state of the art models by showing same efficiency and reliability on detecting single-region and an outperforming for multi-region selective segmentation. Comparison tests were carried out on synthetic and real data images.

Keywords Selective segmentation · Multi-region segmentation · Variational model · Active contours · edge extraction

A. Haider
Department of Mathematics, University of Peshawar, Pakistan
E-mail: dr.haider@uop.edu.pk

Sh. Faisal
Department of Mathematics, University of Peshawar, Pakistan
E-mail: sfaisaluop@gmail.com

K. Chen
Department of Mathematical Sciences, University of Liverpool, UK
E-mail: k.chen@liverpool.ac.uk

L. Rada
Biomedical Engineering Department, Bahcesehir University, Turkey
E-mail: lavdie.rada@eng.bau.edu.tr

1 Introduction

Image segmentation, which is the process of extracting objects from their surroundings in a given image, have been extensively studied and successfully implemented in different fields in the last decades. Global segmentation, where the contour of all the objects in a given image is required to be segmented, is the first explored image segmentation class. Global segmentation aims a distinguish of the foreground and background in a given image [2,3,9,14,16,17]. In this category, threshold and histogram analysis [44,34,50] were followed by region-growing [1,57], edge detection [16,5,29] and active contours region-based techniques [16], etc.. Region-based variational segmentation techniques [15,16] prove to be very efficient for extracting homogeneous areas and segment the boundaries of the object in a given image compared with other models mentioned above. As an alternative to region-based variational segmentation techniques, statistical methods [19,23,45], etc., are known for their ability in segmenting inhomogeneous images. The above-mentioned segmentation models segment the boundaries of all the objects/ features in the given image. The second category requires a particular segmentation of an object of interest in a given image typically used to partition the given image into regions that are in some sense homogeneous or have some semantic significance. The task of interactive /selective segmentation is the detection of an object of interest given some additional information such as location or geometric constraints, thus providing information about scene structure. The technique used to solve such a problem vary from distributions probability, edge detection function, graph cut theory, continuous-domain convex active contour [25,43,26,11,27,24,55,36,8, 40,13,46,20,32,41], etc. One of the distinguished model as a state of art was introduced by Nguyen et al. [36], competing with previous methods such as [43,51]. Nguyen et al. [36] model combine geometric points outside and inside the objects with a continuous-domain convex active contour toward the correct segmentation of an aimed object. Even though the model works for single and multiple regions interactive/ selective segmentation cannot handle transparent or semi-transparent boundaries. Nguyen et al. [36] method works properly under the assumption that the object is smooth and can be well described by the weighed shortest boundary length which limits the validity of the method in a wide range of applications. Other important works, such as superpixel segmentation clustering algorithms [28,47] or different energies functions ideas [46,21,39,52,48] for a satisfactory graph cut solution, has been introduced in the last years. Even though there is a wide range of recent introduced interactive methods there are still problems occurring with under or over-segmentation of the object of interest. This is due to the fact that interactive/ selective segmentation in difference with global segmentation has additional particular task of correct boundary segmentation for homogeneous and non-homogeneous objects, localization of the object of interest, noise robustness, ability to segment multi-region objects as a single object of interest, as well as avoidance of trivial solutions.

Parallel with the unsupervised mentioned methods supervised methods have been introduced as an alternative. Supervised segmentation techniques have been broadly investigated in the last decades in machine learning and pattern recognition. Different algorithms in deep learning, especially convolutional networks [12,30,6,18,31], have been introduced. However, their large training sets makes them limited by the lack of generalization to previously unseen object classes, and can not demonstrate sufficient accuracy for images with poor quality and intensity inhomogeneity [56]. An alternative to the above mentioned method was introduced by Gut-LeGuyader-Vese [25,27] followed by Badshah et al. [8], Rada et al. [40], Mabood et al. [33], and Roberts et al. [42] variational selective segmentation methods. Those models combine edge based function, distance functions, intensity constraints with

area-based minimization fitting terms in order to enhance the model's reliability. The latest work of Rada et al. [40] shows an improvement over the Gut-LeGuyader-Vese edge based models [25,27,8] and computes the state of art introduced by Nguyen et al. [36]. Lastly, Roberts et al. [42] work proposed an Chan-Vese reformulation for selective image segmentation which competes the previous work of Nguyen et al. [36]; Rada et al. [40] model; the convex selective segmentation model of Spencer et al. [49] and Liu et al. [32]; submarkov random walks model of Dong et al. [20]. However, all those models are designed as a single-region selective segmentation model and cannot cope with multi-region selective segmentation, as shown in the experimental section.
In this paper, we propose an active contour region based approach which combines edge information and statistical data information with generalized average capable to cope with multiregion selective segmentation. This paper is organized in the following way. Section §2 contains a review of some related works. Section §3 presents our proposed new model and its derived the Euler-Lagrange equation. We describe the discretization of the method and adapt an additive operator splitting (AOS) algorithm for solving the partial differential equation (PDE) which emerges from this problem. In Section §4 we present some experimental results on different data-sets and demonstrate the effectiveness of the proposed method in comparison with the states of art methods such as Nguyen et al. [36] and with the variational model proposed by Rada et al. [40] and Mabood et al. [33]. We conclude the paper in Section §5.

2 A Review of Related Approaches

In the following, we shortly summarize some variational segmentation models related to global and selective/interactive segmentation models. In difference with global segmentation, where all the objects of a given image are aimed to be segmented, the selective/interactive segmentation tends to segment one object/ feature out of the rest of the objects/ features shown in a image scene. One of the most popular region based approaches for global segmentation is introduced by Mumford-Shah [35]. The minimization of the proposed Mumford-Shah [35] functional aims reconstructing a piecewise-smooth function to represent the given original image which would offer the best image segmentation. The proposed model finds edges of a given image by utilizing the smooth piecewise functions that varies over the image domain. Considering the fact that Mumford-Shah model is computationally expensive and complex Chan-Vese (CV) [16] designed a new easy numerically represented model which combines the idea of replacing the piecewise smooth Mumford-Shah function with a piecewise constant function and the level-set representation for intensities inside and outside desired contour. Since the CV model does not utilize image gradient information for the stopping process it can detect contours with or without gradient. Even though this model opened a new path on image segmentation, has its drawbacks on segmenting efficiently images which carry intensity inhomogeneity or texture. To solve such problems lastly, Ali et al. [4] presents a global segmentation model for the segmentation of multiple objects with intensity difference. This model introduces a signed pressure force function based on generalized averages to segment multiple objects in images having maximum and minimum intensity background.

The above mentioned models are for global segmentation because all global features are to be segmented. This model can not cope with cases where a specific object of interest in the given image must be extracted. This particular problem is the task of selective segmentation where additional constraints, such that user inputs marker points to isolate specific objects

of interest, has been applied. Before introducing with our proposed selective segmentation model, which will be capable to extract a particular object of interest having multi-regions, we shortly summarize some selective segmentation models related to our work.

2.1 Selective/ Interactive Segmentation

In this subsection, we will shortly describe some selective/ interactive segmentation method which are related to this work or will be used as comparison models for the following section. We start the revision with a non variational based model followed by some variational based models.

Constrained Active Contours (CAC) Interactive Segmentation Model [36]

Given an input image $I(x,y) : \Omega \to R$ on rectangular domain $\Omega \subset R^2$, Nguyen et al. [36] uses a variation of the random walk approach incorporated into a constrained active contours framework. This model, similar to other selective segmentation work [20,22,43,11,26] uses foreground/background Gaussian mixture models (GMM) as an estimation from the user input. The incorporated the GMM idea into the probability map of the geodesic distances to the foreground/background regions decide on the likelihood that a point (x,y) belongs to the foreground or background.

Area Fitting Edge Enhancement (AFEE) Interactive Segmentation Model [40]

In order to identify features of the object near the set of points in the set $\mathscr{S} = \{(x_i, y_i) : i = 1,2,3,\ldots,m\} \subset \Omega$, placed inside or on the boundaries of an object for the image denoted by $I(x,y)$, Rada et al. [40] used the idea of area fitting term to improve over Gout-LeGuyader-Vese [25,27] and Badshah-Chen model [8]. The model combines an edge enhancement function with two fitting terms which include intensity and region based information. The edge enhancement term in the proposed energy minimization incorporates a $1D$-Hausdorff measure which achieves the minimum energy in the nearest curve to the given set $\mathscr{S}$. The fitting terms of the minimization energy contributes on keeping the area of the segmented region as close as possible to the reference area of the given polygon constructed with the given set $\mathscr{S}$ and as close as possible to the mean intensity of the same polygon.

Textural and Inhomogeneous Object Extraction (TIOE) Interactive Segmentation Model [33]

In the last years, Mabood et al. [33] introduced a new selective segmentation model for segmentation of multiple objects with intensity difference and inhomogeneous. This model employ prior information in terms of geometrical constraints which work in alliance with image information to capture objects with intensity inhomogeneity in a combination with average image of channels (AIC), handling texture and noise. To obtain the AIC, the authors utilize the extended structure tensor (EST) which is an extended version of the classical structure tensor for the texture image segmentation.

For a given gray image $z(x,y)$ the classical structure tensor (CST) J_σ is obtained by Gaussian smoothing of the tensor product of the image gradient, i.e.,

$$J_\sigma = K_\sigma * (\nabla z \nabla z^T) = \begin{pmatrix} K_\sigma * z_x^2 & K_\sigma * z_x z_y \\ K_\sigma * z_x z_y & K_\sigma * z_y^2 \end{pmatrix} \tag{1}$$

where K_σ is a Gaussian kernel with standard deviation σ, and subscripts x and y denote the partial derivatives.

For a grayscale image $z(x,y)$ the extended structure tensor $(EST)J^E_\sigma$ is define as:

$$J^E_\sigma = K_\sigma * (uu^T) = \begin{pmatrix} K_\sigma * z_x^2 & K_\sigma * z_x z_y & K_\sigma * z_x z \\ K_\sigma * z_x z_y & K_\sigma * z_y^2 & K_\sigma * z_y z \\ K_\sigma * z_x z & K_\sigma * z_y z & K_\sigma * z^2 \end{pmatrix} \tag{2}$$

where

$$u = \begin{bmatrix} z_x & z_y & z \end{bmatrix}^T.$$

We clearly can notice that EST expressed in Eq. (2) uses six feature channels instead of three used for CST i.e., z_x^2, z_y^2, and $z_x z_y$. This makes the use of EST more convenient as compared to CST, using in this way the intensity information of the given image. Computed the EST one obtain the AIC, average image of all the channels $J^E_{\sigma,i}(i = 1,2...9)$ belonging to the EST J^E_σ. The AIC denoted by $z^\star$ is given by

$$z^\star = \frac{1}{9}\sum_{i=1}^{9} J^E_{\sigma,i} \tag{3}$$

where σ is the standard deviation of Gaussian kernel.

Taking into consideration this knowledge, TIOE interactive segmentation minimization functional for selective segmentation is given as follows:

$$F^{2D}_{TIOE} = \mu \int_\Omega d(x,y) g\Big(|\nabla z|\Big)\delta(\phi)|\nabla\phi| dxdy + \lambda D(z^\star(x,y)). \tag{4}$$

The first term in the above functional contains information on the edge distance to the given set of points whereas the second term is the data term which uses the information from the AIC to tackle textural and noisy object of interest. In order to have a suitability of the data fitting term the term $D_{term}(z^\star(x,y))$ (4) has been considered in three different option 1) $D_{constant}$, 2) D_{CoV}, and 3) D_{linear}. The data term $D_{constant}$ performs better with detecting homogeneous intensity objects and is robust against noise [7], however, its performance is poor in images with intensity inhomogeneity. The data term D_{CoV} is good in detecting objects with diffuse edges and objects with unilluminated intensities [10]. However, this data term is also not efficient in images with intensity inhomogeneity whereas the data term D_{linear} performs well in images with intensity inhomogeneity.

Geodesic Distance Minimization (GDM) Interactive Segmentation Model [42]

Lastly, Roberts et al. [42] introduced a reformulation of Chan-Vese model for a convex selective segmentation task by improving over the previous work of Roberts et al. [41]. They proposed an improved on the old selective model by using geodesic distance from the given marker set as the distance term combined with a new function which gives information on the background intensity. The proposed model incorporates the edge function into the curve detection as well as in a edge weighted epsilon-neighborhood fitting term. In this way the model avoids the dependence on the background intensity.

3 A New Multi-region Selective Segmentation Model

This section presents the proposed selective segmentation method, which combines three main elements in the design of the energy functional:

1. the generalized average fitting terms, used to improve the reliability of the model for multi region selective segmentation
2. an edge-detector function, which minimizes the energy in the boundary
3. a prior terms which guaranty that the volume area of each object remains close to a reference area
4. a distance function which has an important role for critical cases where the boundaries are extremely weak

Given a set $\mathscr{S} = \{(x_i, y_i) : i = 1, 2, 3, \ldots, m\} \subset \Omega$, containing geometrical points taken nearby the boundaries of an object/ objects in a given image $I(x,y)$, the energy minimization functional of the proposed model is given as follows:

$$\begin{aligned} E(G_{a_1}, G_{a_2}, \Gamma) = \mu \int_{\Gamma} d(x,y) g(|\nabla I(x,y)|) dxdy + \lambda_1 \int_{inside(\Gamma)} |I(x,y) - G_{a_1}|^2 dxdy \\ + \lambda_2 \int_{outside(\Gamma)} |I(x,y) - G_{a_2}|^2 dxdy + \nu \Bigg\{ \left(\int_{inside(\Gamma)} dxdy - A_1 \right)^2 \\ + \left(\int_{outside(\Gamma)} dxdy - A_2 \right)^2 \Bigg\}, \end{aligned} \tag{5}$$

where $\mu \geq 0$, $\lambda_1 \geq 0$, $\lambda_2 \geq 0$, and $\nu \geq 0$, are given constants, g is an edge detection function given by:

$$g(|\nabla u_0(x,y)|) = \frac{1}{1 + k|\nabla u_0(x,y)|^2}, \text{ for } k \text{ a positive constant} \tag{6}$$

$d(x,y)$ is a distance function defined as:

$$d(x,y) = \text{distance}((x,y), \mathscr{S}) = \prod_{i=1}^{n_1} \left(1 - e^{-\frac{(x - x_i^*)^2}{2\tau^2}} e^{-\frac{(y - y_i^*)^2}{2\tau^2}} \right), \tag{7}$$

$\forall (x,y) \in \Omega$, and $(x_i^*, y_i^*) \in \mathscr{S}$ A_1, A_2 are areas inside and outside the initial polygon respectively, G_{a_1} represents the known generalized mean of the polygon constructed with the help of markers and G_{a_2} gives the generalized mean intensity outside the desired object defined as:

$$G_{a_1}(\phi) = \frac{\int_{\Omega} I^{\alpha}(x,y) u(\phi) dxdy}{\int_{\Omega} I^{\alpha-1}(x,y) u(\phi) dxdy}, \qquad G_{a_2}(\phi) = \frac{\int_{\Omega} I^{\alpha}(x,y)(1 - u(\phi)) dxdy}{\int_{\Omega} I^{\alpha-1}(x,y)(1 - u(\phi)) dxdy} \tag{8}$$

where I is the given image, $\alpha \in \mathbb{R}$. The value of the parameter α varies between $\alpha > 1$ and $\alpha < 1$ for images of maximum intensity background and minimum intensity background, respectively [4]. This term resembles the generalized statistical intensity information which lead to a derivation of the truly contours of the objects. We easily can notice that for $\alpha = 1$ the generalized mean intensity terms will represent the CV model whereas for $\alpha = \pm\infty$, the terms of the generalized mean intensity approach the maximum and minimum intensity in the foreground and background of the image, respectively. The tuning of the parameter α provides a deviation from the intensity to the mean value of the foreground and background. This property equips the proposed model with two terms which has the capability on varying

the intensity value for the foreground and background, leading to a great use in selective segmentation cases.

Analyzing the proposed energy function in Eq. (5) we can notice that the first term is a weighted length term, the second and third term denotes the region fitting terms based on a generalized average and fourth and fifth terms are a prior fitting terms stating that the volume area of the objects inside the polygone constructed with the given markers and outside it remains close to the reference area.

Rewriting the above equation in terms of the level set formulation we have:

$$\begin{aligned} E(a_2,\phi) = \mu \int_\Omega d(x,y)g(|\nabla I(x,y)|)\delta_\varepsilon(\phi)|\nabla\phi|dxdy + \lambda_1 \int_\Omega |I(x,y)-G_{a_1}|^2 H_\varepsilon(\phi)dxdy \\ +\lambda_2 \int_\Omega |I(x,y)-G_{a_2}|^2 (1-H_\varepsilon(\phi))dxdy + \nu\Bigg\{\left(\int_\Omega H_\varepsilon(\phi(x,y))dxdy - A_1\right)^2 \\ +\left(\int_\Omega (1-H_\varepsilon(\phi(x,y)))dxdy - A_2\right)^2\Bigg\}, \end{aligned} \tag{9}$$

with H_ε the regularized Heaviside function considered similar to the works [16,17,37,38]:

$$H_\varepsilon(w) = \frac{1}{2}\left(1+\frac{2}{\pi}\arctan(\frac{w}{\varepsilon})\right), \quad \text{with} \quad \delta(\phi) = H'(\phi) = \frac{\varepsilon}{\pi(\varepsilon^2+w^2)},$$

in order fix the handicap of the non differentiability at the origin of the well known $H-$Heaviside function.

Minimizing Eq. (9) with respect to ϕ by keeping G_{a_1} and G_{a_2} fixed, we get the following Euler Lagrange equation:

$$\begin{aligned} \delta_\varepsilon(\phi)\Bigg\{\mu\nabla.\left(W\frac{\nabla\phi}{|\nabla\phi|}\right) - \lambda_1\left(I(x,y)-G_{a_1}\right)^2 + \lambda_2\left(I(x,y)-G_{a_2}\right)^2\Bigg\} \\ -\ \delta_\varepsilon(\phi)\nu\Bigg\{\left(\int_\Omega H_\varepsilon dxdy - A_1\right) - \left(\int_\Omega (1-H_\varepsilon)dxdy - A_2\right)\Bigg\} = 0 \quad \text{in } \Omega \end{aligned} \tag{10}$$

where $W(x,y) = d(x,y)g(|\nabla I|)$ and $\frac{\partial\phi}{\partial\mathbf{n}} = 0$ on $\partial\Omega$ the Neumann boundary condition for the problem. To speed up the convergence of the evolving level set function a balloon term such as $\varepsilon W|\nabla\phi|$ can be added. The final equation is written as:

$$\begin{aligned} \delta_\varepsilon(\phi)\Bigg\{\mu\nabla.\left(W\frac{\nabla\phi}{|\nabla\phi|}\right) - \lambda_1\left(I(x,y)-G_{a_1}\right)^2 + \lambda_2\left(I(x,y)-G_{a_2}\right)^2\Bigg\} \\ -\delta_\varepsilon(\phi)\nu\Bigg\{\left(\textstyle\int_\Omega H_\varepsilon dxdy - A_1\right) - \left(\int_\Omega (1-H_\varepsilon)dxdy - A_2\right)\Bigg\} - \varepsilon W|\nabla\phi| = 0 \end{aligned} \tag{11}$$

The above equation can be approximated by involving artificial time step t which leads to the following evolution equation:

$$\begin{aligned} \frac{\partial\phi}{\partial t} = \delta_\varepsilon(\phi)\Bigg\{\mu\nabla.\left(W\frac{\nabla\phi}{|\nabla\phi|}\right) - \lambda_1\left(I(x,y)-G_{a_1}\right)^2 + \lambda_2\left(I(x,y)-G_{a_2}\right)^2\Bigg\} \\ -\ \delta_\varepsilon(\phi)\nu\Bigg\{\left(\int_\Omega H_\varepsilon dxdy - A_1\right) - \left(\int_\Omega (1-H_\varepsilon)dxdy - A_2\right)\Bigg\} - \varepsilon W|\nabla\phi| = 0, \end{aligned} \tag{12}$$

with Neumann boundary conditions.

An Additive Operator Splitting Algorithm for a Fast Solution of the Proposed Method

In order to solve Eq. (12), we need a fast convergent numerical method which has low computational cost. One such numerical method is the additive operator splitting (AOS) method introduced by Weickert [54]. In this method, a two dimensional problem is decomposed into two one-dimensional ones. We first discretize Eq. (12) which results in a semi-implicit linear system and then design a numerical scheme for solving tridiagonal linear system which is diagonally dominant.

Considering Eq. (12) with initial level set $\phi(x,y,0)=\phi_0(x,y)$, and $|\nabla\phi|_\gamma=\sqrt{\phi_x^2+\phi_y^2+\gamma}$ a replacement for $|\nabla\phi|$ in order to avoid singularities, for γ a small constant and

$$\begin{aligned} f &= \delta_\varepsilon(\phi)\Big\{-\lambda_1\big(I(x,y)-G_{a_1}\big)^2+\lambda_2\big(I(x,y)-G_{a_2}\big)^2\Big\} \\ &- \delta_\varepsilon(\phi)\nu\Big\{\Big(\int_\Omega H dxdy-A_1\Big)-\Big(\int_\Omega(1-H)dxdy-A_2\Big)\Big\}-\varepsilon W|\nabla\phi|, \end{aligned} \tag{13}$$

with $F=\frac{W}{|\nabla\phi|_\gamma}$, Eq. (12) takes the form:

$$\frac{\partial\phi}{\partial t}=\begin{cases}\mu\delta_\varepsilon(\phi)\nabla.(F\nabla\phi)+f= \\ \mu\delta_\varepsilon(\phi)\nabla.(\partial_x(F\partial_x\nabla\phi))+\partial_y(F\partial_y\nabla\phi)+f\end{cases} \tag{14}$$

Eq(12) takes the following matrix-vector form by discretizing the spatial step.

$$\frac{\phi^{n+1}-\phi^n}{\Delta t}=\sum_{l=1}^{2}A_l(\phi^n)\phi^{n+1}+f(x,y),$$

where Δt represents time step size, n is the n^{th} iteration and A_l gives the quantity of diffusion in l-direction (in two dimensional case, $l=1$ and $l=2$ shows x and y direction respectively). The semi-implicit form of the above equation is

$$\phi^{n+1}=\Big[I-\Delta t\sum_{l=1}^{2}A_l(\phi^n)\Big]^{-1}\hat{\phi^n}\quad\text{for } l=1,2\quad\text{and}\quad\hat{\phi^n}=\phi^n+\Delta t f(x,y)$$

which can be split additively by applying AOS scheme as given below in order to define the AOS solution

$$\phi^{n+1}=\frac{1}{2}\sum_{l=1}^{2}\Big[I-2\Delta t A_l(\phi^n)\Big]^{-1}\hat{\phi^n} \tag{15}$$

The matrices A_l, for $l=1,2$ represent tridiagonal matrices which have been derived by using finite differences.

$$\begin{aligned} \Big(A_l(\phi^n)\phi^{n+1}\Big) &= \mu\delta_\varepsilon(\phi^n)\Big(\partial_x\big(F\partial_x\phi^{n+1}\big)\Big)_{i,j} \\ &= \mu\delta_\varepsilon(\phi^n)\frac{F^n_{i+1/2,j}\big(\partial_x\phi^{n+1}\big)^n_{i+1/2,j}-F^n_{i-1/2,j}\big(\partial_x\phi^{n+1}\big)^n_{i-1/2,j}}{h_x} \\ &= \mu\delta_\varepsilon(\phi^n)\frac{\frac{F^n_{i+1,j}+F^n_{i,j}}{2}\Big(\frac{\phi^{n+1}_{i+1,j}-\phi^{n+1}_{i,j}}{h_x}\Big)-\frac{F^n_{i,j}+F^n_{i-1,j}}{2}\Big(\frac{\phi^{n+1}_{i,j}-\phi^{n+1}_{i-1,j}}{h_x}\Big)}{h_x} \end{aligned}$$

$$= \mu\delta_\varepsilon(\phi^n)\frac{F^n_{i+1,j}+F^n_{i,j}}{2h_x^2}\left(\frac{\phi^{n+1}_{i+1,j}-\phi^{n+1}_{i,j}}{h_x}\right) - \mu\delta_\varepsilon(\phi^n)\frac{F^n_{i,j}+F^n_{i-1,j}}{2h_x^2}\left(\frac{\phi^{n+1}_{i,j}-\phi^{n+1}_{i-1,j}}{h_x}\right),$$

in the same manner we get,

$$\left(A_2(\phi^n)\phi^{n+1}\right) = \mu\delta_\varepsilon(\phi^n)\left(\partial_y\left(F\partial_y\phi^{n+1}\right)\right)_{i,j}$$

$$= \mu\delta_\varepsilon(\phi^n)\frac{F^n_{i,j+1/2}\left(\partial_y\phi^{n+1}\right)^n_{i,j+1/2} - F^n_{i,j-1/2}\left(\partial_y\phi^{n+1}\right)^n_{i,j-1/2}}{h_y}$$

$$= \mu\delta_\varepsilon(\phi^n)\frac{\frac{F^n_{i,j+1}+F^n_{i,j}}{2}\left(\frac{\phi^{n+1}_{i,j+1}-\phi^{n+1}_{i,j}}{h_y}\right) - \frac{F^n_{i,j}+F^n_{i,j-1}}{2}\left(\frac{\phi^{n+1}_{i,j}-\phi^{n+1}_{i,j-1}}{h_y}\right)}{h_y}$$

$$= \mu\delta_\varepsilon(\phi^n)\frac{F^n_{i,j+1}+F^n_{i,j}}{2h_y^2}\left(\frac{\phi^{n+1}_{i,j+1}-\phi^{n+1}_{i,j}}{h_y}\right) - \mu\delta_\varepsilon(\phi^n)\frac{F^n_{i,j}+F^n_{i,j-1}}{2h_y^2}\left(\frac{\phi^{n+1}_{i,j}-\phi^{n+1}_{i,j-1}}{h_y}\right),$$

Algorithm 1 AOS Method Algorithm for Solving the Proposed Method: $\phi^k \leftarrow GMSS(\phi^{(0)}, \mathscr{A}, \mu, \nu, \beta, \alpha, \varepsilon, maxit, \varepsilon, tol)$.

Calculate the edge based function and area of the polygon (distance function optional);
$n = 1$, Compute f from equation (13), $\phi^{(1)} = \phi^{(0)}$;
for $iter = 1 : maxit$ **do**
Compute $\phi^{(n)}$ using (15):

$$\phi_i^{(n+1)} \leftarrow \tfrac{1}{2}\sum_{l=1}^{2}(\,I - 2\Delta t A_l(\phi^n))^{-1}\hat{\phi}^n$$

If $\|\phi^{(n+1)} - \phi^{(n)}\| < tol$ or $iter > maxit$, set $\phi^{(n)} \leftarrow \phi^{(n-1)}$ Break;
else $\phi^{(n)} \leftarrow \phi^{(n-1)}$
update f from equation (13)

end for

4 Experimental Results

This section includes some tests results to illustrate the accuracy and the performance of the proposed model and comparison with the state of art models for selective/interactive segmentation. The experiments are carried out on medical, real and synthetic images. In this section, we show three kinds of experimental results: experiments which validate the correctness of the proposed model; comparison of the proposed model with similar variational models, such as Rada et al. [40] model, Mabood et al. [33] model , and Roberts et al. [42] model for selective segmentation of objects with small intensity difference or deals the objects close to each other; and comparison with nonvariational based models introduced by Nguyen et al. [36]. For convenience we denote:

1. AFEE —the Rada et al. [40] interactive segmentation model;
2. TIOE —the Mabood et al. [33] interactive segmentation model;

3. GDM —the Nguyen et al. [36] interactive segmentation model;
4. CAC —the Roberts et al. [42] interactive segmentation model;

In the following experiments the parameters λ_1, λ_2, ε, Δt, γ, the step size h, and ε have been treated as fixed at $\lambda_1 = \lambda_2 = 1$, $\varepsilon = 1$, $\Delta t = 0.1$, $\gamma = 10^{-6}$, $h = 1$, $\varepsilon = -0.01$, respectively. We emphasize that the distance function is not taken into account in all the results shown in this section, in other words, the distance has been simply considered $d(x,y) = 1$. This function can have a great role in cases where the object aimed to be segmented has a bond with another object of the same intensity. The initial level set has been constructed a sign distant function of the polygon obtained from the given markers. The method has been performed on images having different size in order to show the same satisfactory results. The relative residual 10^{-2} have been used for stopping purposes of the program. We observed that the range of the parameters μ, ν and *power* lie between $\mu = 100$ to $n^2/10$, $\nu = 0.1$ to 1 and $1 < \alpha < 3$ throughout the experiments. The variation α parameter brings flexibility when using this data fitting term in selective formulations on achieving a smaller/larger c_1 value, in other words, α choice has a direct impact on the segmentation of the aimed object. For a better understanding read the note added as the end of this section.

Test set 1-Validation of the Correctness of the Proposed Method and its Comparison with the Rada-Chen Model [40] and Mabood et al. [33] Model

In the first test set, we demonstrate the ability to segment objects which are not piecewise smooth functions. Fig. 1 shows that the proposed method can easily cope with an efficiently selective segmentation of images which have multi-regions within the object. The first column in Fig. 1 shows that AFEE interactive segmentation model [40] is unable to segment the arm included in the body of the given multi-region image. AFEE interactive segmentation model [40] model will not include the arm of this synthetic image as the initial polygon indicates due to the fact that the intensity of the foreground has the same value to the intensity of the arm which makes the AFEE interactive segmentation model [40] model fail. The validity of the new model has been exhibited in the last column of Fig. 1. The second row of this figure contains the same image with an initial level set including the remaining parts of the object. It is evident from the second column on this row that AFEE interactive segmentation model [40] model gives unsatisfactory results by leaving all other parts of the image. The validity of the proposed model was further explored in different images as shown in Fig. 2 and Fig. 3. All those figures are performed on image having multi-regions and small intensity difference among different parts of the image. The last row on which of those figures reveal that the new model algorithm performs well for capturing the object of interest having multi-regions. We can easily observe that the proposed method works quite good with multi-regions real-life image by successfully segmented the aimed object given some points which initialize the initial polygon for the levelset.

Fig. 2 first row shows a successful segmentation of the proposed method in comparison with Rada-Chen [40] and MABCK [33] model. The first row of this figure aims the half-moon in a given image with two reflected half-moons. This row shows satisfactory experimental results of Mabood et al. [33] model, Rada et al. [40] model and our proposed model. The second row of Fig. 2 shows two reflected full-moons with severe intensity change between within the moon image itself. In this row, we see that both Rada et al. [40] model and Mabood et al. [33] model fail to segment such a case whereas the proposed model gives satisfactory results.

Fig. 3 further shows that the models discussed above cannot efficiently segment images which have multi-regions within the object. In this figure we notice that even though Mabood

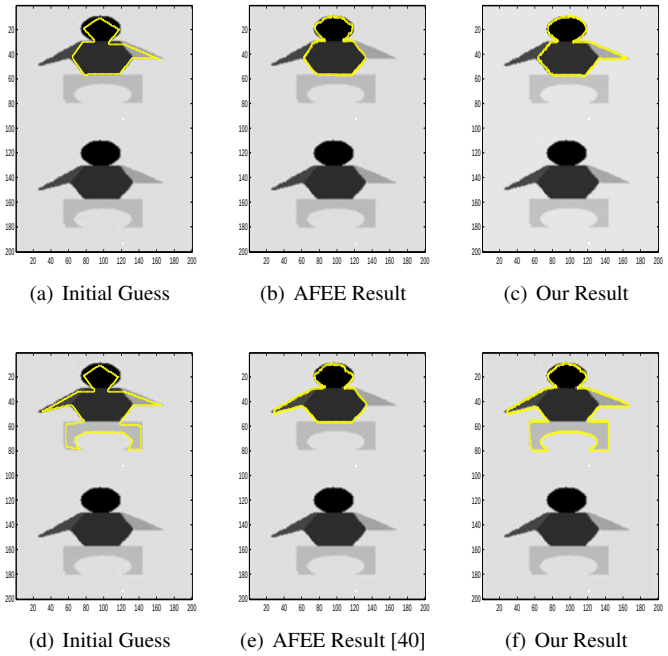

(a) Initial Guess (b) AFEE Result (c) Our Result

(d) Initial Guess (e) AFEE Result [40] (f) Our Result

Fig. 1 Test Set 1-Comparison of the proposed model with Rada-Chen [40] model.

et al. [33] and Rada et al. model [40] are able to successfully segment the desired objects, the contour of the object segmentation distinguishes the multi-region which is not the aim of such kind of problems. Fig. 2 exhibits a multi-regions image of the full moon. The Rada-Chen model model [40] segments the black region successfully and fails to segment the edges and the other half part of the moon. This is to be expected as the model has not been designed for multi-regions images. The Mabood et al. [33] model can deal with color sudden changes but it can be easily noticed there is an instability waving on the edges of the moon as exhibited in Fig. 2 (c), where as the proposed method correctly segments the moon.

In Table 1 we provide the execution time of the proposed method in comparison with Rada et al. [40] and Mabood et al. [33] models for a set of 10 random images size 255×255. The results show a similar speed of the proposed method with Rada et al. [40] method whereas Mabood et al. [33] method performs slower. Through experiments it is observed that Rada et al. [40] model requires more iterations in images with oscillatory boundaries which increases the number of iteration for this method until stopping criteria is satisfied.

Test set 2-Comparison with the Rada-Chen Model [40] and Nguyen et al. [36] Model

We continue our experiments by giving more examples and compare our model with the Nguyen et al. [36] model which is a region merging model and Rada-Chen Model [40] a variational model. Here we show 3 more different images, which can be found as successfully selected by the the proposed method (last column) whereas Rada-Chen Model [40] and Nguyen et al. [36] model shown in the second and the third row, respectively, can not cope properly. Fig. 4 first row, gives unsatisfactory segmentation results for Rada-Chen Model

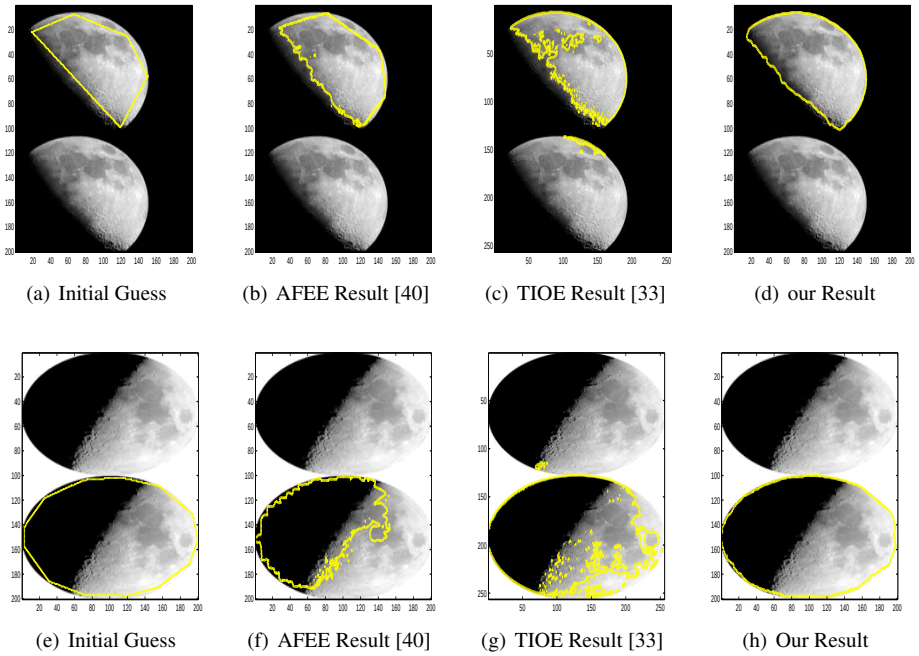

(a) Initial Guess (b) AFEE Result [40] (c) TIOE Result [33] (d) our Result

(e) Initial Guess (f) AFEE Result [40] (g) TIOE Result [33] (h) Our Result

Fig. 2 Test Set 1-Comparison with the Rada-Chen model [40] and MABCK model [33].

Image	proposed model		AFEE		TIOE	
	Iter	CPU	Iter	CPU	Iter	CPU
no : 1	40	7.61473	40	9.23444	70	21.105590
no : 2	30	9.91378	40	17.22647	150	53.09465
no : 3	40	7.61473	50	12.23444	70	21.105590
no : 4	40	7.93433	40	7.6329	70	21.384067
no : 5	40	7.44916	40	6.8750	40	14.826962
no : 8	40	11.57245	60	21.22636	100	41.89010
no : 9	40	7.51556	40	7.74590	40	12.21479
no : 10	50	9.00729	50	9.11530	50	16.00794

Table 1 Efficiency comparison of the proposed, Nguyen et al. [36], Rada et al. [40], Mabood et al. [33] models

[40], which is expected as the edge information conflicts the region information, where as Nguyen et al. [36] model successfully segments both hexagons marked in the given ball. The second row of Fig. 4 shows the image of a palm tree where clearly Rada-Chen Model [40] fails to segment properly the tree and a partial fail of Nguyen et al. [36] has been noticed. The last row of Fig. 4 shows the results of the proposed method which concludes that the model works satisfactorily for cases where the features are nearby and with different shapes. Fig. 4 second row, shows an accurate segmentation on an image of cloths with different color under shade effect, which are considered as much more hard cases due to

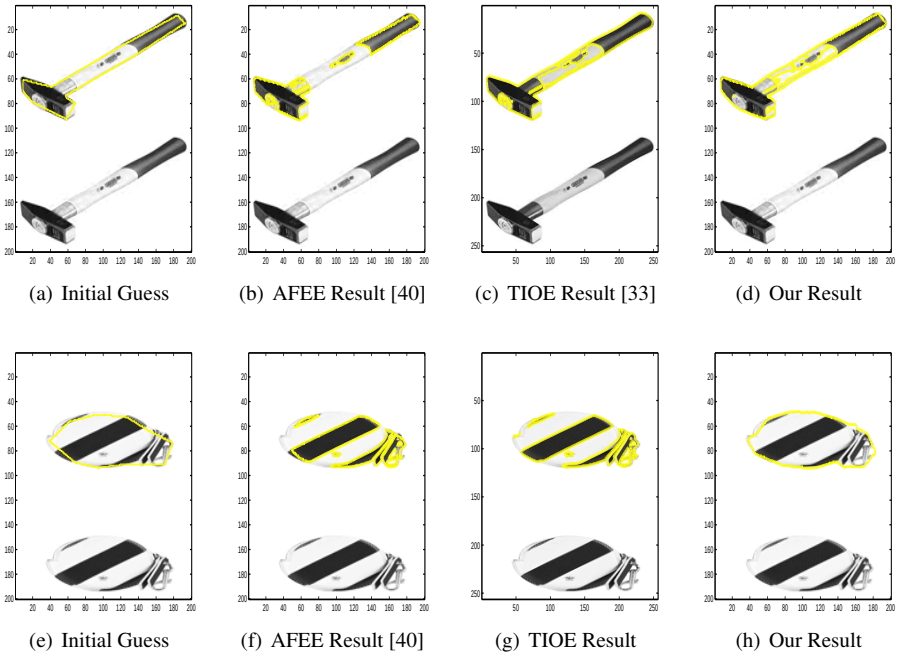

(a) Initial Guess (b) AFEE Result [40] (c) TIOE Result [33] (d) Our Result

(e) Initial Guess (f) AFEE Result [40] (g) TIOE Result (h) Our Result

Fig. 3 Test Set 1-Comparison with MABCK model [33] and the Rada-Chen model [40].

GDM	AFEE	TIOE	Proposed method
0.8 ± 0.074	0.84 ± 0.047	0.7 ± 0.75	0.91 ± 0.083

Table 2 Jaccard similarity coefficients for GDM, AFEE, TIOE and the proposed models.

the multi-region intensity change, low contrast of different features of the given object with respect to the background and the shadow. for cases where the features are nearby and with different shapes. Fig. 4 second row, shows that both Rada-Chen Model [40] and Nguyen et al. [36] model van not successfully cope with such a segmentation

Furthermore, to support the visual results we obtain with the proposed method we also provide the Jaccard similarity coefficients in Table 2 as an quantitative support of the obtained results. The Jaccard similarity coefficient is computed as $J(A,B) = \frac{|A \cap B|}{|A \cup B|}$. The results are obtained from experiments in 20 different images suitable for interactive segmentation with a pre-labeled ground truth consisting of the mean of the labeled ground truth by two different specialist. The results clearly show the superiority of our approach with respect to the approach of Rada et al. [40], Mabood et al. [33] and Nguyen et al. [36] interactive segmentation model. As a general observation, the Rada et al. [40] model produced relatively better results than the Mabood et al. [33] and Nguyen et al. [36] models, but loses details if the image contains high noise or high intensity difference into the aimed object, whereas, the proposed model successfully segments the images by preserving local image details, handling not only severe inhomogeneity but noise as well.

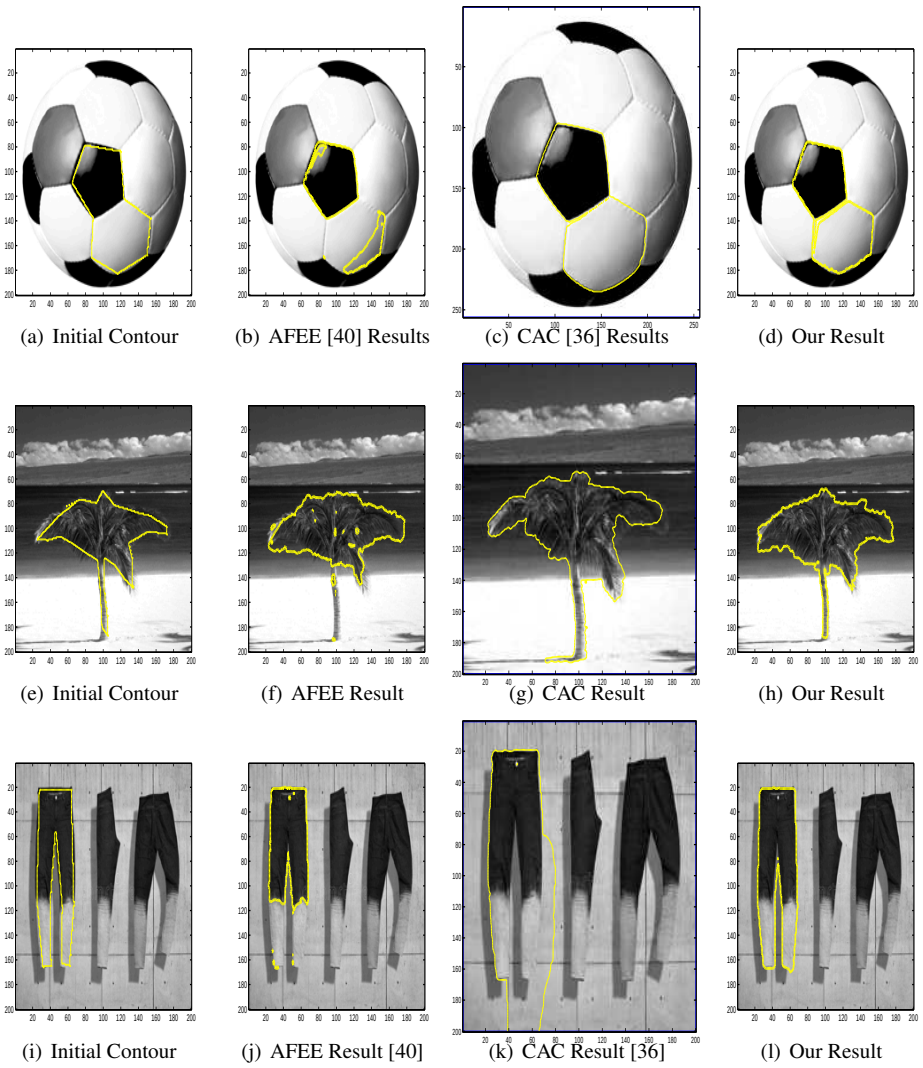

(a) Initial Contour (b) AFEE [40] Results (c) CAC [36] Results (d) Our Result

(e) Initial Contour (f) AFEE Result (g) CAC Result (h) Our Result

(i) Initial Contour (j) AFEE Result [40] (k) CAC Result [36] (l) Our Result

Fig. 4 Test Set 2-Comparison with the Rada-Chen model [40] and Nguyen et al. [36] model.

Testset 3- Hard Dataset Images Including Texture and Medical Image Segmentation. Additional Comparison to Roberts-Spencer Model [42]

Texture images are commonly avoided for selective segmentation task due to their complicated intensity structure. The same occurrence is inherited by real life images which is due to their physical or anatomical conditions. In this section, we show successful segmentation of such hard cases with the proposed model. Fig. 5 shows a synthetic texture image composed by 4 different patterns, followed in the second row by an image of a fish with similar color and pattern with the surrounding corrals, and in the last row show the image of a stack of wood. From the first row the segmentation of the middle placed pattern has been aimed,

from the second row we aim the segmentation of the hidden fish into the corrals, and from the last one we aim the segmentation of one single wood out of the stack. From Fig. 5, it is observed that Rada-Chen model [40], shown in the second column, will not segment those objects as one single object but as a structure with varying levels. In a similar way, Fig. 6 shows CT scan images where accurate segmentation of the cancer region is required. The segmentation of the cancer region is hard due to the intensity difference into the region as well as the intensity similarity with the scull. From Fig. 6 last column we can easily see that the proposed method successfully segments the desired part of the brain while the results shown in this figure on the second and third column show that the compared models can not accurately segment the desired part. In both Fig. 5 and 5 the initai given points has been reflected in the image output.

Before concluding this section we are adding some more comparison results of the proposed model with Roberts-Spencer model [42] which showed better performance in medical image selective segmentation compared with previous work of Nguyen et al. [36], Rada and Chen [40] model, Spencer–Chen [49] model, Liu et al. [32] model, and Dong et al. [20] model. The result obtained from this model are shown in Fig. 7. We can clearly see that this model fails segmenting inhomogeneous or multilevel object aimed for the selective segmentation task. This has to be expected as this model and most of other models already shown above as their are designed as a single-region selective segmentation model.

Note. Similar to other inverse problems there is always discussion on details behind tuning parameters and the initialization input points. This drawback has been inherited to the output results of our method shown in this work as they are reliant on user input and parameter tuning. We would like to further discuss on two main inputs which makes significant output changes, user input points and the parameter α tuning. The input points should be as close as possible to the aimed objects such that the area A_1 of the constructed polygon is close to the real segmented object. To avoid the user input, toward an automatic selective segmentation, different characteristic of the objects can be considered and implemented, similar to the work of Roberts and Spencer [42] where the class of CT organs is aimed. Another drawback of the proposed model is its dependence on the parameter α used to calculate the generalized average. For a better understanding on how the parameter α will influence the segmentation results we show an example with different value of α, Fig. 8. In this example, we vary the parameter α in the set $[-1,0,1,2,3]$. The variance of the α directly influence c_1 value by increasing or decreasing it. Fig. 8 shows the image of brain in which we can notice the dominance of dark gray intensity. The main aim of this experiment is to capture the cancer region which clearly is not homogeneous. As the region of interest is a combination of white gray scale and open gray scale having a big α means higher value for the c_1 mean average, which is not the aim of this problem. Fig. 8 shows clearly that for $\alpha > 0$ we have a increment of the segmentation of white gray scale of the aimed region of interest rather the whole cancer itself. In this particular case, small value of α will decrease the c_1 value, which will include a wider region including the combined values of white gray scale and open gray scale into a single average. Our future work consist on an automatic selection for the parameter α related to the intensity of the given polygon placed over the aimed object to be segmented. However, we would like to emphasize that the benefit of the proposed approach is that the parameters can be chosen depending on the test set class under the consideration rather then a generalized case as it was considered in this framework.

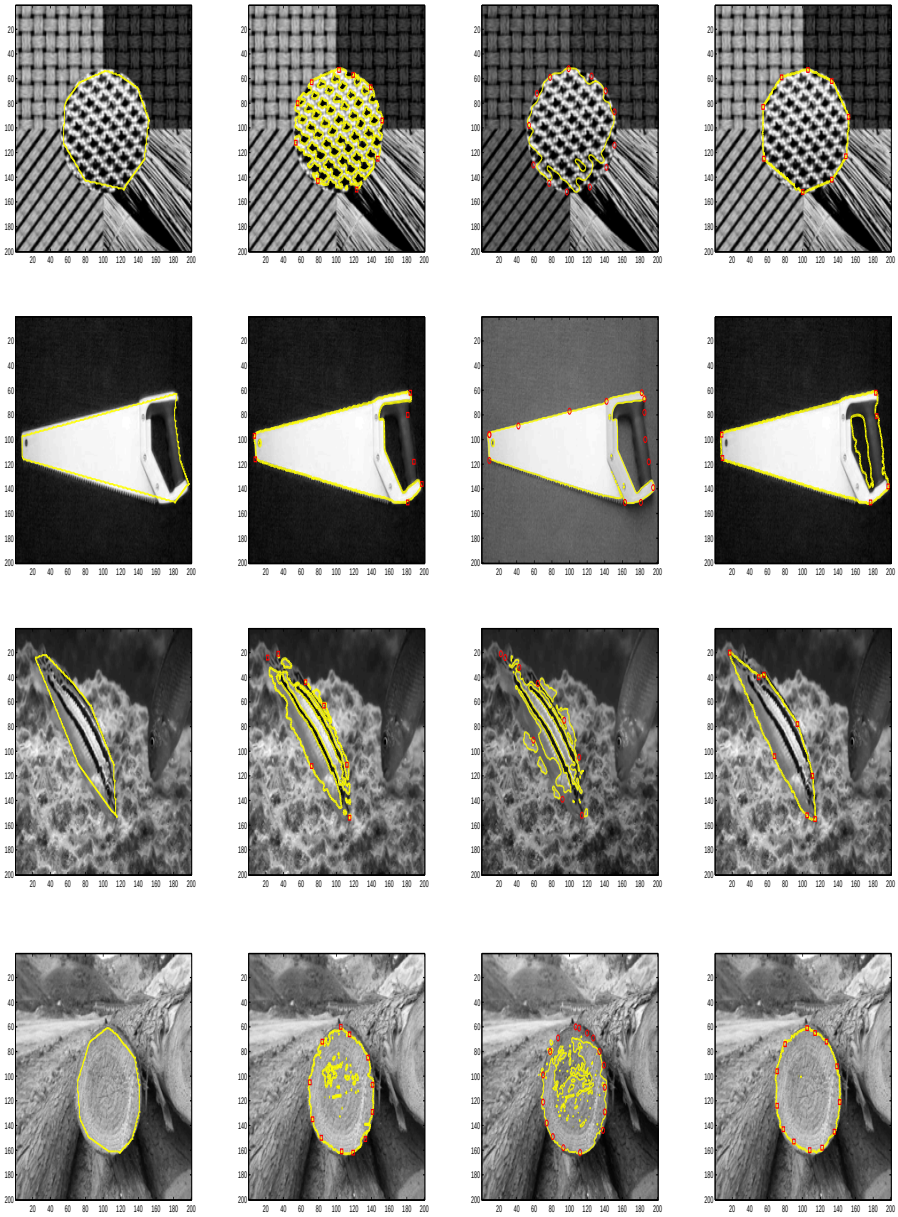

(a) Initial contour (b) AFEE Result [40] (c) TIOE Result [33] (d) Our Result

Fig. 5 Successful result of the proposed model, shown in the last column, in comparison with Rada et al. [40] model, second column, Mabood et al. [33] model, third column.

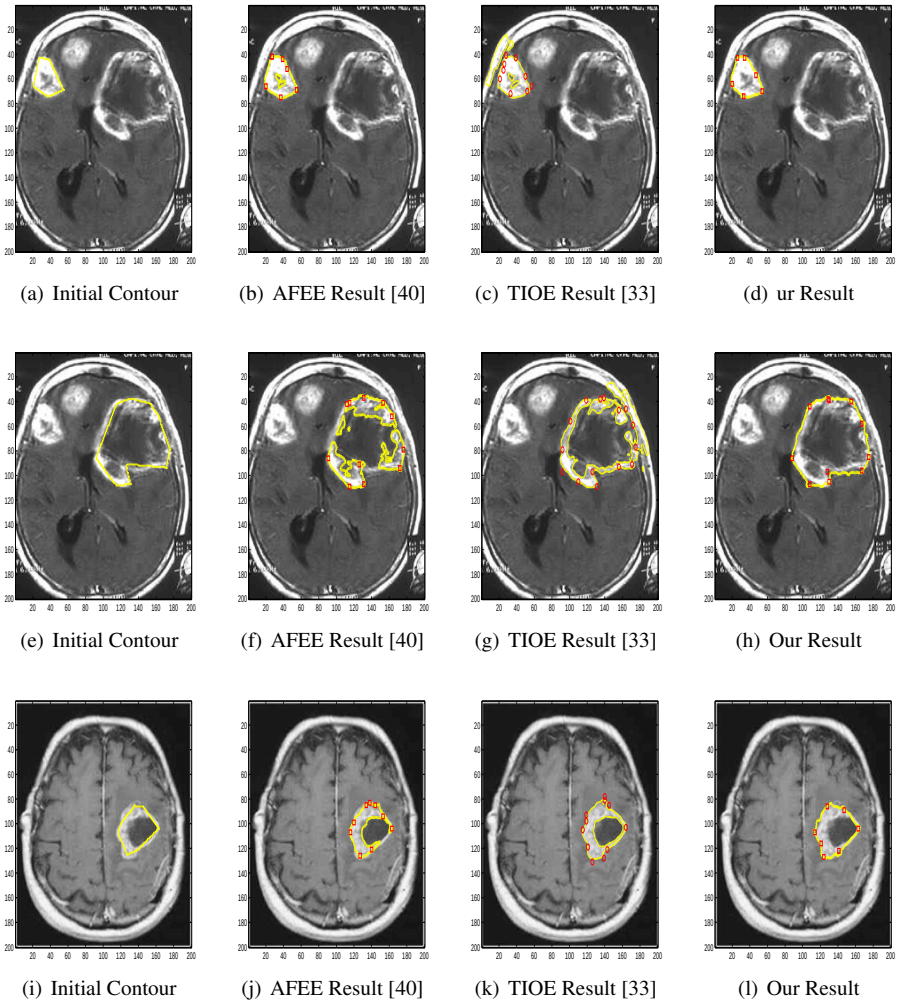

(a) Initial Contour (b) AFEE Result [40] (c) TIOE Result [33] (d) ur Result

(e) Initial Contour (f) AFEE Result [40] (g) TIOE Result [33] (h) Our Result

(i) Initial Contour (j) AFEE Result [40] (k) TIOE Result [33] (l) Our Result

Fig. 6 Successful result of the proposed model, shown in the last column, in comparison with Rada et al. model [40], second column, Mabood et al. [33] model, third column.

5 Conclusion and Future Work

In this research work, we developed a new model for selective segmentation of images which is capable to extract a particular object of interest having multi-regions. Moreover, we compared our results with the Rada et al. [40], Mabood et al. [33], Roberts at al. [42], and Nguyen et al. [36] models. From the experimental results, we found that the proposed model is more efficient in segmenting an aimed objects or feature in comparison with those of traditional models for selective segmentation. The promising results of this work will be further extended for harder cases such as inhomogeneous images with multi-region intensity in presence of high noise, unsupervised single dominant object estimation in a given video sequence of color images using similar ideas to the work of Wang et al. [53]. An illustration

Fig. 7 Unsuccessful result of the Roberts-Spencer model [42] for inhomogeneous and multi-level segmentation.

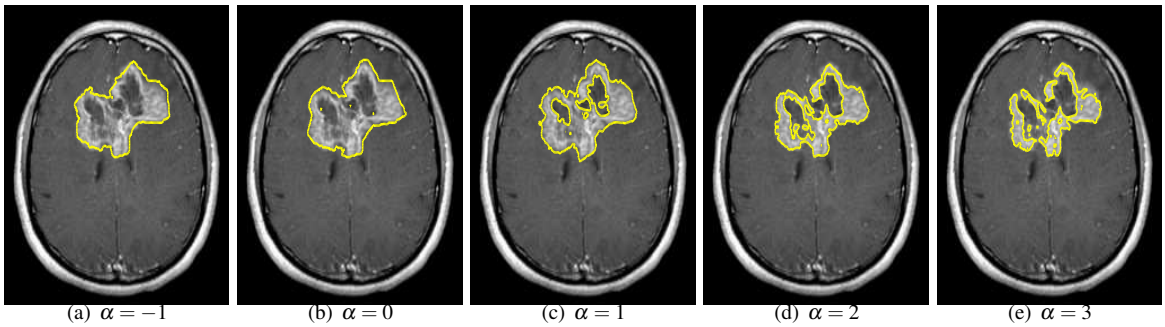

(a) $\alpha = -1$ (b) $\alpha = 0$ (c) $\alpha = 1$ (d) $\alpha = 2$ (e) $\alpha = 3$

Fig. 8 Results obtained of the proposed model for varying the parameter α.

of such case it is shown in Fig. 9 where the aimed object has at least three main distinctive regions in presence of blur and noise.

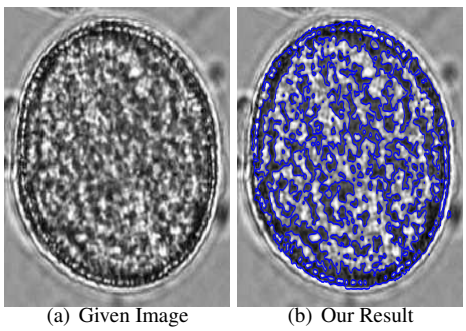

(a) Given Image (b) Our Result

Fig. 9 Fail cases of the proposed model.

6 Compliance with Ethical Standards

Conflict of Interest: Author Ali Haider declares that he has no conflict of interest. Author Shah Faisal declares that he has no conflict of interest. Author Ke Chen declares that he has no conflict of interest. Author Lavdie Rada declares that she has no conflict of interest.

References

1. Adams, R., Bischof, L.: Seeded region growing. IEEE Transactions on Pattern Analysis and Machine Intelligence **16**(6), 641–647 (1994). DOI 10.1109/34.295913. URL http://dx.doi.org/10.1109/34.295913
2. Akram, F., Kim, J.H., Lim, H.U., Choi, K.N.: Segmentation of intensity inhomogeneous brain mr images using active contours. Comput. Math. Methods. Med. **51**, 1 – 14 (2014)
3. Ali, H., Badshah, N., Chen, K., Khan, G.A.: A variational model with hybrid images data fitting energies for segmentation of images with intensity inhomogeneity. Pattern Recognition **51**, 27 – 42 (2016). DOI https://doi.org/10.1016/j.patcog.2015.08.022. URL http://www.sciencedirect.com/science/article/pii/S0031320315003106
4. Ali, H., Zikria, N., Badshah, N., Chen, K., Khan, G.A.: Multiphase segmentation based on new signed pressure force functions and one level set function. Turkish Journal of Electrical Engineering and Computer Science **25**, 2943 – 2955 (2017)
5. Aubert, G., Kornprobst, P.: Mathematical Problems in Image Processing: Partial Differential Equations and the Calculus of Variations, 2nd edn. Springer Publishing Company, Incorporated (2010)
6. Badrinarayanan, V., Kendall, A., Cipolla, R.: Segnet: A deep convolutional encoder-decoder architecture for image segmentation. CoRR **abs/1511.00561** (2015). URL http://arxiv.org/abs/1511.00561
7. Badshah, N., Chen, K.: Image selective segmentation under geometrical constraints using an active contour approach. Commun. Comput. Phys. **7**(4), 759–778 (2009)
8. Badshah, N., Chen, K.: Image selective segmentation under geometrical constraints using an active contour approach. Math. Comput. **7**, 759–778 (2010)
9. Badshah, N., Chen, K., Ali, H., Murtaza., G.: Coefficient of variation based image selective segmentation model using active contours. East Asian Journal on Applied Mathematics **2**(2), 150–169 (2012)
10. Badshah, N., Chen, K., Ali, H., Murtaza., G.: Coefficient of variation based image selective segmentation using active contour. East Asian Journal on Applied Mathematics **2**, 150–169 (2012)
11. Bai, X., Sapiro, G.: A geodesic framework for fast interactive image and video segmentation and matting. IEEE International Conference on Computer Vision pp. 1–8 (2007)
12. Brostow, G.J., Fauqueur, J., Cipolla, R.: Semantic object classes in video: A high-definition ground truth database. Pattern Recogn. Lett. **30**(2), 88–97 (2009). DOI 10.1016/j.patrec.2008.04.005. URL http://dx.doi.org/10.1016/j.patrec.2008.04.005
13. Cai, X., Chan, R., Zeng, T.: A two-stage image segmentation method using a convex variant of the mumford–shah model and thresholding. SIAM Journal on Imaging Sciences **6**(1), 368–390 (2013)
14. Caselles, V., Kimmel, R., Sapiro, G.: Geodesic active contours. International Journal of Computer Vision **22**(1), 61–79 (1997). DOI 10.1023/A:1007979827043. URL https://doi.org/10.1023/A:1007979827043
15. Chan, T.F., Vese, L.A.: Active contours without edges. CAM Report, UCLA pp. 98–53 (1998)
16. Chan, T.F., Vese, L.A.: Active contours without edges. IEEE Transactions on Image Processing **10**(2), 266–277 (2001). DOI 10.1109/83.902291
17. Chen, K.: Matrix Preconditioning Techniques and Applications. Cambridge Monographs on Applied and Computational Mathematics. Cambridge University Press (2005). DOI 10.1017/CBO9780511543258
18. Chen, L.C., Papandreou, G., Kokkinos, I., Murphy, K., Yuille, A.L.: Deeplab: Semantic image segmentation with deep convolutional nets, atrous convolution, and fully connected crfs. IEEE Transactions on Pattern Analysis and Machine Intelligence **40**(4), 834–848 (2018). DOI 10.1109/TPAMI.2017.2699184
19. Comaniciu, D., Meer, P.: Mean shift: A robust approach toward feature space analysis. IEEE Transactions on Pattern Analysis and Machine Intelligence **24**, 603–619 (2002)
20. Dong, X., Shen, J., Shao, L.: Submarkov random walk for image segmentation. IEEE Transactions on Image Processing **25**(2), 516–527 (2016)
21. Dong, X., Shen, J., Shao, L., Yang, M.: Interactive cosegmentation using global and local energy optimization. IEEE Transactions on Image Processing **24**(11), 3966–3977 (2015). DOI 10.1109/TIP.2015.2456636
22. Falcao, A., Udupa, J., Migazawa, F.: An ultrafast user-steered image segmentation paradigm: live wire on the fly. IEEE Transactions on Medical Imaging **19**(1), 55–62 (2002)

23. Geman, S., Geman, D.: Stochastic relaxation, gibbs distributions and the bayesian restoration of images. IEEE Transaction on Pattern Analysis and Machine Intelligence **6**, 721–741 (1984)
24. Goldstein, T., Bresson, X., Osher, S.: Geometric applications of the split bregman method: Segmentation and surface reconstruction. J. Sci. Comput. **45**, 272–293 (2010)
25. Gout, C., Guyader, C.L., Vese, L.A.: Segmentation under geometrical consitions with geodesic active contour and interpolation using level set methods. Numerical Algorithms **39**, 155–173 (2005)
26. Grady, L.: Random walks for image segmentation. IEEE Trans. Pattern Anal. Mach. Intell. **28**(11), 1768–1783 (2006). DOI 10.1109/TPAMI.2006.233. URL http://dx.doi.org/10.1109/TPAMI.2006.233
27. Guyader, C.L., Gout, C.: Geodesic active contour under geometrical conditions theory and 3d applications. Numerical Algorithms **48**, 105–133 (2008)
28. H. Li, W.W., Wu, E.: Robust interactive image segmentation via graph-based manifold ranking. Comp. Visual Media **1**, 183–195 (2015). DOI https://doi.org/10.1007/s41095-015-0024-2
29. Kass, M., Witkin, A., Terzopoulos, D.: Snakes: Active contour models. International Journal of Computer Vision **1**(4), 321–331 (1988). DOI 10.1007/BF00133570. URL https://doi.org/10.1007/BF00133570
30. L, Z., Y, G., Y, X.: Representative discovery of structure cues for weakly-supervised image segmentation. IEEE Transactions on Multimedia **16**(2), 470–479 (2014)
31. Litjens, G., Kooi, T., Bejnordi, B.E., Setio, A.A.A., F. Ciompi, M.G., van der Laak, J.A., Ginneken, B.V., Sanchez, C.I.: A survey on deep learning in medical image analysis. Medical Image Analysis **42**, 60–88 (2017)
32. Liu, C., Ng, M., Zeng, T.: Weighted variational model for selective image segmentation with application to medical images. Pattern Recognition **76**, 367–379 (2018)
33. Mabood, L., Ali, H., Badshah, N., Chen, K., Khan, G.A.: Active contours textural and inhomogeneous object extraction. Pattern Recognition **55**, 87 – 99 (2016). DOI https://doi.org/10.1016/j.patcog.2016.01.021. URL http://www.sciencedirect.com/science/article/pii/S003132031600042X
34. Malik, J., Leung, T., Shi, J.: Contour and texture analysis for image segmentation. International Journal of Computer Vision **43**, 7–27 (2001). DOI 10.1023/A:1011174803800. URL http://dl.acm.org/citation.cfm?id=543015.543016
35. Mumford, D., Shah, J.: Optimal approximation by piecewise smooth functions and associated variational problems. Communications on Pure Applied Mathematics **42**, 577–685 (1989)
36. Nguyen, T.N.A., Cai, J., Zhang, J., Zheng, J.: Robust interactive image segmentation using convex active contours. IEEE Transactions on Image Processing **21**, 3734–3743 (2012)
37. Osher, S., Fidkew, R.: γ-level set methods and dynamic implicit surfaces. In:2003 Lecture notes in Comp Sci, Springer Verlag. **3708** (2005)
38. Osher, S., Sethian, J.A.: Fronts propagating with curvature-dependent speed: Algorithms based on hamilton-jacobi formulations. Journal of Computational Physics **79**(1), 12 – 49 (1988). DOI https://doi.org/10.1016/0021-9991(88)90002-2. URL http://www.sciencedirect.com/science/article/pii/0021999188900022
39. Peng, J., Shen, J., Li, X.: High-order energies for stereo segmentation. IEEE Transactions on Cybernetics **46**(7), 1616–1627 (2016). DOI 10.1109/TCYB.2015.2453091
40. Rada, L., Chen, K.: Improved selective segmentation model using one level-set. Journal of Algorithms and Computational Technology **7**, 506–540 (2013)
41. Roberts, M., Chen, K., Irion, K.: A convex geodesic selective model for image segmentation. Journal of Mathematical Imaging and Vision **61**(4), 482–503 (2019)
42. Roberts, M., Spencer, J.: Chan–vese reformulation for selective image segmentation. Journal of Mathematical Imaging and Vision pp. 1–24 (2019). DOI https://doi.org/10.1007/s10851-019-00893-0
43. Rother, C., Kolmogorov, V., Blake, A.: Grabcut: Interactive foreground extraction using iterated graph cuts. ACM SIGGRAPH **23**(3), 1–6 (2004)
44. Sen, D., Pal, S.K.: Histogram thresholding using fuzzy and rough measures of association error. Image Processing, IEEE Transactions on **18**(4), 879–888 (2009). DOI 10.1109/TIP.2009.2012890
45. Shen, J., Dong, X., Peng, J., Jin, X., Shao, L., Porikli, F.: Submodular function optimization for motion clustering and image segmentation. IEEE Transactions on Neural Networks and Learning Systems **30**(9), 2637–2649 (2019). DOI 10.1109/TNNLS.2018.2885591
46. Shen, J., Du, Y., Li, X.: Interactive segmentation using constrained laplacian optimization. IEEE Transactions on Circuits and Systems for Video Technology **24**(7), 1088–1100 (2014). DOI 10.1109/TCSVT.2014.2302545
47. Shen, J., Hao, X., Liang, Z., Liu, Y., Wang, W., Shao, L.: Real-time superpixel segmentation by dbscan clustering algorithm. IEEE Transactions on Image Processing **25**(12), 5933–5942 (2016). DOI 10.1109/TIP.2016.2616302

48. Shen, J., Peng, J., Dong, X., Shao, L., Porikli, F.: Higher order energies for image segmentation. IEEE Transactions on Image Processing **26**(10), 4911–4922 (2017). DOI 10.1109/TIP.2017.2722691
49. Spencer, J., Chen, K.: A convex and selective variational model for image segmentation. Commun. Math. Sci. **13**(6), 1453–1472 (2015)
50. Vincent, L., Soille, P.: Watersheds in digital spaces: An efficient algorithm based on immersion simulations. IEEE Transactions on Pattern Analysis and Machine Intelligence **13**, 583–598 (1991). DOI http://doi.ieeecomputersociety.org/10.1109/34.87344
51. W. Yang J. Cai, J.Z., Luo, J.: User-friendly interactive image segmentation through unified combinatorial user inputs. IEEE Trans. Image Process. **19**(9), 2470–2479 (2010)
52. Wang, W., Shen, J.: Higher-order image co-segmentation. IEEE Transactions on Multimedia **18**(6), 1011–1021 (2016). DOI 10.1109/TMM.2016.2545409
53. Wang, W., Shen, J., Yang, R., Porikli, F.: Saliency-aware video object segmentation. IEEE Transactions on Pattern Analysis and Machine Intelligence **40**(1), 20–33 (2018). DOI 10.1109/TPAMI.2017.2662005
54. Weickert, J., Romeny, B.M.T.H., Viergever, M.A.: Efficient and reliable schemes for nonlinear diffusion filtering. IEEE Transactions on Image Processing **7**(3), 398–410 (1998). DOI 10.1109/83.661190
55. Zhang, K., Zhang, L., Song, H., Zhou, W.: Active contours with selective local or global segmentation: a new formulation and level set method. Image and Vision Computing **28**(4), 668–676 (2010)
56. Zhao, F., Xie, X.: An overview of interactive medical image segmentation. Annals of the BMVA **2013**, 1–22 (2013)
57. Zucker, S.W.: Region growing: childhood and adolescence. Computer Graphics and Image processing pp. 382–399